Spatially structured host genetic diversity leads to the evolution of local specialization

Elisa Visher[1,2], Anisha Ali[3,4], Jonathan Barajas[3], Sehar Masud[3], Annika McBride[3], Edwin Ramos[3], Melissa Sui[3,5], Cristina Villalobos-Heredia[3], Natalie Walzer[3], P. Signe White[1], Mike Boots[1]

1 Department of Integrative Biology, University of California, Berkeley, CA, 94720, USA

2 Department of Genetics, Stanford University, Stanford, CA, 94305, USA

3 University of California, Berkeley, CA, 94720, USA

4 Department of Psychology, Cal State East Bay, CA, 94542, USA

5 Department of Plant and Microbial Biology, University of California, Berkeley, CA, 94720, USA

ABSTRACT

Host heterogeneity and spatial population structure each influence parasite evolution but may also interact because space structures contacts between host types. Here, we experimentally evolve granulosis virus in microcosms of its *Plodia interpunctella* (Indian meal moth) host that differ in both spatial structure and host genetic diversity. We control spatial structure by manipulating the viscosity of the food that the larvae live within and host genetic diversity by adding larvae from either a single or two inbred lines to opposite ends of the microcosm. We preserve spatial structure across passages and assay virus from different positions within the microcosm on both host genotypes. We find that the lower contact rates between host genotypes resulting from spatial structure can lead to the evolution of locally specialized virus, even when the host population is genetically diverse overall. We also find that spatial structure changes how viruses specialize: viruses evolved in well-mixed environments had lower exploitation of familiar hosts, while those in spatially structured environments exhibited higher exploitation of familiar hosts. These results demonstrate that spatial structure and host heterogeneity interact to shape pathogen specialization and that the evolutionary consequences of host diversity depends on the population structure.

Keywords: *experimental evolution, host range evolution, spatial structure, virus evolution, virulence, disease ecology and evolution, trade-offs*

INTRODUCTION

A body of literature on the 'monoculture effect' has shown that host genetic diversity affects infectious disease dynamics in both ecological and evolutionary contexts [1–5]. Specifically, genetically diverse host populations can decrease the prevalence of infectious diseases and may constrain their evolution of transmissibility or virulence [3,6–12]. This can be explained by heterogeneous host populations limiting the transmission of specialist pathogens and thereby selecting for 'mediocre' generalists that may be constrained by costs associated with expanded niche breadth [13–19]. This theory, however, only considers scenarios where the genetic diversity of the host population is well-mixed so that transmission occurs readily between host types. However, it is clear that many host populations exhibit some sort of spatial or contact network structuring. In this case, a parasite lineage may be more likely to infect one host type even if the population is genetically diverse overall. The impact of this interaction between host genetic diversity and spatial population structure on the evolution of pathogens is not well understood.

Several theoretical studies have examined the impact of spatial structure by manipulating the contact matrix between hosts to show that the degree of mixing in a population should change the evolutionarily optimal strategy for host range [20–22]. Higher contact rates between host types select for generalists in simple models [20–22], but can theoretically also lead to greater specialization when migration increases the amount of genetic variation that selection can act upon or increases local competition for patches [23–25]. Additionally, spatially structured transmission may impose additional selection pressures beyond the effect on host type mixing. Theory and experiments show that more local transmission results in 'self-shading' that can select for less infective, more prudent pathogens due to both genetic and ecological correlations that arise in spatial populations [26–34], though intermediate spatial structure can also select for higher exploitation rates [28,33]. Finally, these host range trade-offs and life history trade-offs may interact. Theory considering multidimensional trade-offs has shown that interactions between trade-offs of different classes can produce evolutionary outcomes that deviate from the predictions of single trade-off models [35–37]. This means that how organisms evolve to specialize or may also depend on the selective pressures acting on other trade-offs [35].

There are, therefore, many open questions for how we expect spatial structure and host genetic diversity to interact, both in terms of how host type mixing affects host range evolution and also in terms of how these different selection pressures interact. We explore these interactions by experimentally evolving granulosis virus in microcosms of its *Plodia interpunctella*, or Indian meal moth (Hübner), host that vary in their host genetic diversity and spatial structuring. We alter host heterogeneity by adding larvae from either the same or different inbred populations (host genotypes) to either half of the microcosm [38] (Figure 1). We manipulate spatial structure by altering the viscosity of the food medium that larvae live within [30,39,40]. Food viscosity therefore both manipulates the contact rates between hosts and structures infectious contacts [20,30]. The treatments are then fully crossed so that each host treatment is in both food viscosity treatments. Our experiment therefore explores how spatial structure and host heterogeneity interact and how the spatial structuring of heterogeneity affects its impact on pathogen evolution. We demonstrate that spatially

structured host heterogeneity can promote local specialization and constrain the evolution of generalist viruses. Moreover, altering the spatial structure of a population changes how specialization affects pathogen traits. Specifically, the direction of specialization's effect on host exploitation rate—whether pathogens exhibit higher or lower exploitation on their familiar host compared to a foreign host—depends on the spatial structure under which they evolved.

METHODS

Study system

Plodia interpunctella, or the Indian meal moth, is a stored grain pest that naturally lives at high population density within its cereal food medium for 5 larval instar stages before it pupates into an adult moth that disperses, mates, and lays eggs, but does not eat [41,42]. It has a semelparous, monthly cyclical life cycle where the population moves through life stages roughly concordantly [40]. It is naturally infected by the *Plodia interpunctella* granulosis virus (PiGV), a dsDNA baculovirus that transmits when larvae directly cannibalize infection killed cadavers or consume virus that was released into the environment from such cadavers [43,44]. Thus, the virus is an obligate killer that will only transmit if it kills its host. Notably, the virus can only infect *P. interpunctella* during the larval stages and, if exposed larvae clear the infection, they can pupate and carry out the rest of their life history as normal [45]. Infection killed cadavers are recognizable because successful infection turns larvae an opaque, chalky white color due to the high density of viral occlusion bodies [46]. The system has proved a powerful tool for examining the effects of spatial structure on pathogen exploitation rates and, more recently, host genotype specialization [30,38].

Host genotype selection and maintenance

For this experiment, we selected two inbred populations of *P. interpunctella* that were previously generated in the lab by brother-sister mating individuals for >27 generations [47]. Each population should therefore be essentially a clonal population of two distinct host genotypes (Genotype 9 and Genotype 17). These genotypes were chosen because they had similar levels of general resistance or, alternatively worded, the ancestral virus has similar levels of initial infectivity on them [38] (Table S2, Figure S3). We have previously shown that virus evolved in homogeneous populations of these specific host genotypes can specialize on its familiar host genotype by increasing their infectivity and/or productivity [38].

We maintained these genotypes as inbred lines in wide-mouthed Nalgene pots (ThermoFisher Scientific, U.K.) in the absence of infection with 200g 'Standard' food medium (made in batches of 500g cereal mix (50% Earth's Best oatmeal, 30% wheat bran, 20% rice flour), 100g brewer's yeast, 2.2g sorbic acid, 2.2g methyl paraben, 125ml honey, and 125ml glycerol) in incubators set at 27±2 °C and 35±5% humidity, with 16:8hr light: dark cycles [48]. To maintain populations, ~50 adult moths were moved into a new pot with new food when they emerged monthly. Thus, host lines were maintained in the absence of infection and did not evolve throughout the experiment.

Manipulating spatial structure

We manipulated spatial structure in the experiment by changing the viscosity of the food medium as in [30,39,40]. Because larvae live within their food medium, this alters individuals' dispersal patterns and thus the spatial structure of their infectious contacts. We made food of two viscosities, 'loose' and 'sticky', which differ solely in the amount of glycerol added. 'Loose' food contains 500g Earth's Best oatmeal, 100g brewer's yeast, 2.2g sorbic acid, 2.2g methyl paraben, and 175ml glycerol. 'Sticky' food contains 500g Earth's Best oatmeal, 100g brewer's yeast, 2.2g sorbic acid, 2.2g methyl paraben, and 450ml glycerol. 'Loose' and 'sticky' food was then added to wide-mouthed Nalgene pots and frozen overnight to kill any insect eggs potentially contaminating the food. The mass of food added to these pots (300g 'loose' and 550g 'sticky' food) was determined by the volume needed to entirely fill half of one of our plastic microcosm containers.

We tested the impact of food viscosity on spatial structure in several ways. First, we measured life history traits (development time and mass at pupation) of larvae added to assay grids with 'sticky' and 'loose' food (as in [48]) to ensure that food viscosity did not affect these metrics (Figure S1). Second, we added 'loose' and 'sticky' food to 4 cm diameter PVC pipes (10 each), added 11-day old 3rd instar larvae to one side of the pipe, and measured how far larvae dispersed after 10 days (Table S1). Finally, we set up microcosms with the two food types as in our experiment below but added food containing larvae to only one half of the microcosm and sterile food to the other half. We incubated these microcosms for 21 days, then recorded the position of every individual (Figure 2A).

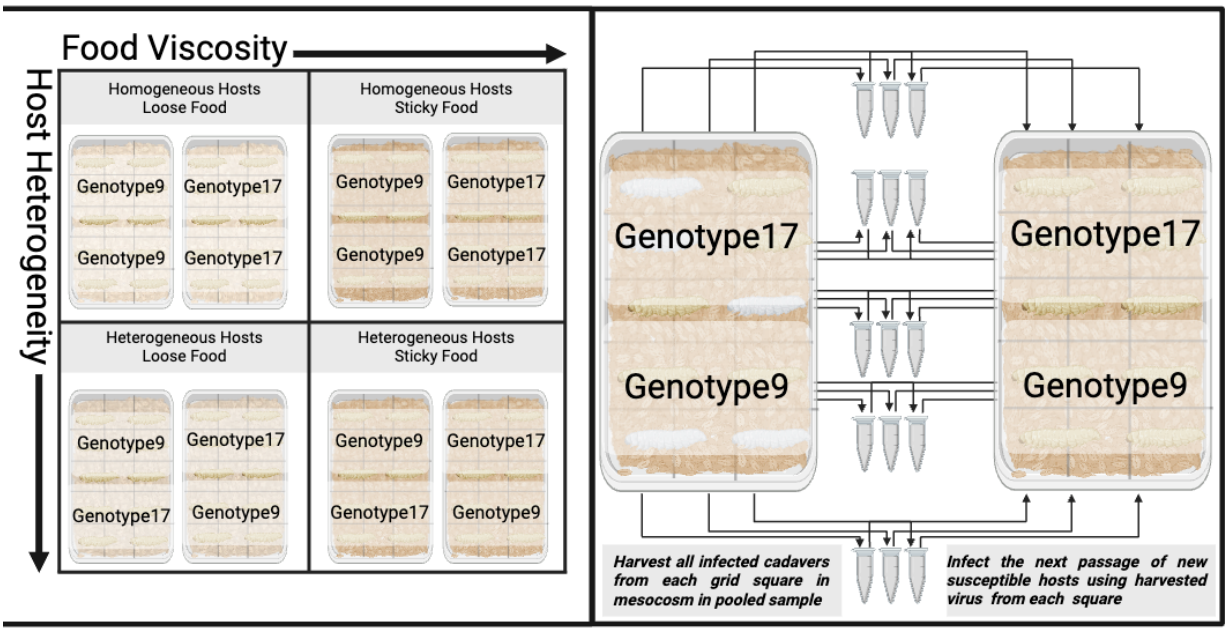

Figure 1: Experimental design and passaging scheme. (Left) Each microcosm was set up by adding 2 pots of food containing 11-day old larvae to opposite vertical ends of a plastic microcosm with a 3x5 grid. The 3rd row of the grid is therefore a contact zone between the hosts. There are 3 replicates for each of the 8 microcosms. There are 4 different treatment types of homogeneous or heterogeneous hosts by 'loose' or 'sticky' food. Each homogeneous treatment was set up with both host types and each heterogeneous host treatment was set up alternating which host was on 'top' or 'bottom' of the grid. Microcosms were consistently oriented in the growth chamber so that the

'bottom' side was closer to the door. (Right) After 20 days incubating with virus, microcosms were frozen and dissected into grid squares. All infected larvae from each grid square were harvested, added to a 1.5mL Eppendorf tube (1 square per tube), and homogenized to release occlusion bodies. 500mL of the virus solution was then pipetted in droplets over the same grid square of a new microcosm of the same treatment set-up with fresh 11-day old hosts. Therefore, the spatial force of infection was preserved across passages. We experimentally evolved virus for 10 passages.

Setting up host populations for microcosms

After thawing the pots of 'sticky' and 'loose' food, we added ~50 similarly aged adult moths to each pot from either our Genotype 9 or Genotype 17 host maintenance populations and incubated them for 10 days. These single-genotype adults mated and laid eggs into the 'sticky' or 'loose' food. 10 days after adding adults, these pots were used to set up microcosms as in Figure 1. While pots were set up with the same number of adults, they may not have contained the same number of larvae. Observationally, population sizes may have varied from a couple dozen individuals to mid-hundreds of individuals.

Microcosms were set up in 9.25" x 12.08" x 0.9" inch plastic A4 document cases (Daiso Japan, U.S.A.) that had been marked with an even 3 x 5 grid of 3.08" x 2.42" squares. We set up 8 microcosms per replicate: 1) homogeneous Genotype 9 hosts in 'loose' food; 2) homogeneous Genotype 17 hosts in 'loose' food; 3) homogeneous Genotype 9 hosts in 'sticky' food; 4) homogeneous Genotype 17 hosts in 'sticky' food; 5) heterogeneous hosts (Genotype 9 on top / Genotype 17 on bottom) in 'loose' food; 6) heterogeneous hosts (Genotype 17 on top / Genotype 9 on bottom) in 'loose' food; 7) heterogeneous hosts (Genotype 17 on top / Genotype 9 on bottom) in 'sticky' food ; and 8) 7) heterogeneous hosts (Genotype 9 on top / Genotype 17 on bottom) in 'sticky' food (Figure 1). Each microcosm therefore had a single food type (either 'sticky' or 'loose'), according to its treatment.

To arrange hosts in the microcosm, we added 2 pots of the food containing 10-day old larvae to opposite vertical ends of the grid, so that food fully filled the plastic containers. For homogeneous host treatments, we added 2 pots containing larvae of the same genotype and, for heterogeneous treatments, these 2 pots contained larvae of different genotypes. Thus, homogeneous genotype microcosms had a single genotype of host throughout the grid, while heterogeneous microcosms had two genotypes separated vertically across the grid with a contact zone at the 3rd row. To balance our treatments and account for potential effects due to position within the grid, we set up 2 microcosms of each of the 2 heterogeneous treatments and alternated which genotype is on 'top'.

These microcosms were then incubated overnight, as above, so that virus could be added to them on day 11. We repeated this process each passage to set up new microcosms so that evolving virus were added to a fresh microcosm. This allowed us to maintain 2 non-interbreeding and non-evolving host genotypes in our microcosms and preserve the spatial structuring of such genotypes across passages.

Experimental evolution

We set up 3 replicates of each of our 8 unique microcosm types (24 serially passaged microcosms total). We initiated serial passage by pipetting 5ml of 10^{-2} stock virus solution in

186 small droplets evenly over the top of each microcosm. Each microcosm was then incubated for
187 20 days and then frozen overnight to kill larvae for harvesting. Passage lengths (10 days before
188 set-up, 1 day overnight, 20 days with virus) therefore roughly correspond to the host's natural
189 ~monthly cyclical demography [40]. The average 'time to kill' for the ancestral virus on third
190 instar larvae is ~15.5 days (range 6-24), so this also roughly corresponds to a natural infection
191 cycle (Figure S2). We stagger the replicates' passaging schedules weekly due to the time
192 intensive nature of passaging.

193 To harvest virus, we dissected each microcosm by grid square and separately collected infection
194 killed cadavers from each square in sterile 1.5ml Eppendorf tubes (Figure 1). We added 1ml
195 sterile, MilliQ water to each square's tube and used a sterile pellet pestle (Fisher Scientific,
196 U.S.A.) to manually burst larvae and release viral occlusion bodies. We dropleted 500ul of this
197 solution from each square onto the same square of that treatment's freshly set-up microcosm
198 to infect the next passage and froze the rest of the solution. Therefore, we preserved the force
199 of and spatial structure of infection within the grid across passages. We recorded the number
200 of infected cadavers in each square at each passage to track the spatial ecology of infection in
201 the experiment.

202 The microcosms newly infected with passaged virus were then placed back into incubators for
203 20 days to allow the virus to infect larvae for the next passage. During this time, larvae disperse
204 from their initial position at a rate determined by their food viscosity, ingest virus from the sites
205 they move between, and carry their infection to their eventual site of death. This means that
206 larvae in heterogeneous sticky food microcosms are both less likely to become infected by virus
207 from the alternate host type and are less likely to move across the contact zone to infect the
208 alternate host type. We experimentally evolved virus for 10 passages, a number standard for
209 microbial evolution experiments.

210 There were several occasions where we had to use the frozen virus solutions reserved during
211 passaging to re-set up passages due to low numbers of infected cadavers or contamination with
212 another pathogen. Low infected numbers were caused by low total population sizes and tended
213 to happen in batches when a set of adults did not breed for whatever reason. There were no
214 observable trends in when this would occur. Bt contamination was much rarer and also tended
215 to happen in batches (potentially when a food batch had been contaminated) without
216 observable trends. Contamination was recognizable because the most common contaminant,
217 *Bacillus thuringiensis* (Bt), turns infected larvae black rather than white [49]. We could generally
218 expect any co-infected larvae to display the black phenotype since Bt kills larvae more quickly
219 (Yitbarak, unpublished data), so re-setting up passages when Bt was visually detected would
220 clear the virus population and prevent co-infection from selecting on evolving virus.
221 Congruously, we did not see any signs of persistent contamination within our passages nor in
222 any of our assays.

223 <u>Assay</u>

224 After passage 10, we collected virus infected cadavers from each square as above. We next
225 pooled the virus from the 3 squares in each row of the 3x5 grid in equal proportion so that we
226 had 5 virus samples per microcosm. Each pooled sample was therefore the virus population at a
227 certain vertical position within the microcosm, along the gradient of heterogeneity for the

228 heterogeneous host microcosms. We purified virus by centrifuging for 1 min at 3000 rpm to
229 remove larger particulate matter and then 3 min at 13000 rpm to pellet virus. We ran these
230 samples through a .65 micron filter to semi-purify our virus of larger bacterial and fungal
231 contaminants, as in [38]. Next, we quantified the concentrations of each sample by counting
232 occlusion bodies on a Petroff-Hauser counting chamber with 400x darkfield microscopy and
233 diluted each to an assay dose concentration of ~7.5x10^8 occlusion bodies per mL in 2%
234 sucrose and .2% dye [38]. The sugar entices the larvae to ingest the virus and the dye allows the
235 experimenter to determine which have ingested half their body lengths of solution and are
236 considered exposed.

237 We assayed each pooled virus sample on both of our two host genotypes, Genotype 9 and
238 Genotype 17, in a balanced, batched design (see Table S3) to determine the proportion of hosts
239 each virus sample infects on each genotype and the average number of occlusion bodies each
240 virus sample produces per infection on each genotype. With 5 virus samples for each of the 8
241 microcosms that have 3 replicates, this resulted in 240 virus sample x assay genotype
242 combinations. Because only 1 genotype is assayed per day and there are strong day effects
243 within the system, we included assay genotype and set-up date in all statistical models to
244 account both for any general differences in resistance and assay day effects. Furthermore,
245 conclusions are drawn from comparing the relative phenotypes of evolved virus on the
246 different assay genotypes rather than comparing to the ancestral population that was assayed
247 separately (Figure S3, Table S2).

248 To set up infectivity assays, we first moved ~70-80 adult moths of the appropriate host
249 genotype into new pots with 200g 'standard' food. Eleven days after setting up assay pots, we
250 collected 100 third instar larvae for each assay combination in a petri dish and starved them
251 under a damp paper towel for 2 hours. After starvation, we syringed tiny droplets of the
252 appropriate virus-sucrose-dye solution onto the petri dish for the larvae to consume. We added
253 50 larvae that have orally ingested half their body lengths of virus solution to 2 25-cell
254 compartmentalized square petri dishes (ThermoFisher Scientific, U.S.A.) with 'standard' food
255 and incubated them for 20 days [38]. Assay grids were labelled with random identifiers to blind
256 assay combinations and prevent bias. After 20 days, assay grids were frozen and destructively
257 sampled to count the number of infected and uninfected individuals. Infected cadavers from
258 each assay grid were then saved in a pooled sample for virus quantification.

259 To determine the average number of occlusion bodies produced per infected individual, we
260 extracted virus from the pooled samples from each assay grid using a sterile pellet pestle
261 (Fisher Scientific, U.S.A.) to manually burst larvae and release viral occlusion bodies. We then
262 centrifuged these samples as above, but did not filter them, and counted occlusion bodies on a
263 Petroff-Hauser counting chamber. The concentration of occlusion bodies was then divided by
264 the number of infected cadavers that were in the pooled sample to get the average number of
265 occlusion bodies produced per infection for each virus sample on each host genotype.

266 Statistical analyses

267 We analyzed our data using a generalized linear mixed modelling framework in R [50]. All
268 models were run in R version 4.2.3 (2023-03-15) -- "Shortstop Beagle" [51]. We used packages
269 'glmmTMB' and 'lme4' to build models, 'DHARMa' to check model residuals, 'afex' and 'car' to

270 determine significant model terms, 'emmeans' to extract effects, 'tidyverse' to manipulate
271 data, and 'patchwork' and 'ggplot2' to plot results [52–60]. We determined error structures for
272 models by testing fitted models with 'DHARMa' and then adjusting to best fit residuals. On
273 occasion, observation level random effects were used to correct overdispersion in our models
274 [61]. Where necessary, contrasts were used with 'emmeans' to determine effect estimates for
275 treatments. All model tables and annotated code are in the supplement. Models are numbered
276 in the table (MS, M1-6) with suffixes indicating the response variable being tested (i for
277 infectivity, p for productivity, and c for composite exploitation rate) and referenced in the
278 manuscript as appropriate.

279 Spatial structure analysis

280 First, we analyzed how larvae moved in our microcosm food viscosity test (Figure 2A) by asking
281 whether the total count of individuals in a square is predicted by an interaction between the
282 viscosity of the food and the distance (in square number) that the square is from where larvae
283 were added (with squares where larvae were directedly added coded as 0) (MS2). The model
284 uses a Poisson error structure with observation level random effects.

285 We next examined how food viscosity spatially structured infection during the evolution
286 experiment using the data collected on the number of infected individuals in each square at
287 each passage for each microcosm. To do this, we ran a Levene's Test for Homogeneity of
288 Variance on the infected count data to determine if our 'sticky' and 'loose' food treatments
289 differ in their variance, a measure of how 'clumpy' infection is within a microcosm (MS1).

290 Assay analysis

291 Infectivity and productivity assay data were analyzed in a generalized linear mixed modeling
292 framework using the same packages and process as above [50]. We built models treating
293 proportion infected, average number of occlusion bodies per infected individual, and the
294 composite exploitation rate (proportion infected multiplied by the average virus count) as our
295 response variables. We transformed average virus counts and composite exploitation rates by
296 multiplying and rounding them to produce integer counts for Poisson and negative binomial
297 distribution assumptions. In each model, we included random effects for batch and the nested
298 effect of virus sample under replicate under treatment.

299 First, we asked whether there are significant interaction effects between the genotype that the
300 virus is being assayed on, the host treatment that the virus is from, and the spatial structure
301 that the virus is from by building models with a three-way interaction between these terms
302 (M1). To more closely look for trends in our data, we asked whether virus populations
303 significantly differ in their specialization at the whole microcosm level by building models that
304 include an interaction effect between the assay being on the host that the population was
305 evolved on ('familiar') or the foreign host and the type of food the population evolved in (M2).
306 Virus from heterogeneous populations was coded as 'heterogeneous' as they do not have a
307 familiar or foreign host at the whole microcosm level. We also included assay genotype as a
308 fixed effect to account for any overall differences in resistance between our assay host
309 genotypes. Model convergence issues prevented us from including the evolution genotype in all
310 models, but, since this term had very weak effects ($p>0.9$) in the models that did converge, we

311 dropped the term to improve comparability across models. The infectivity model uses a
312 binomial error structure with observation level random effects, the productivity model uses a
313 Poisson error structure with observation level random effects, and the exploitation rate model
314 uses a zero-inflated negative binomial error structure with observation level random effects. To
315 better see the effects of specialization in the homogeneous populations, we also ran these
316 same models for the homogeneous host treatments only with the infectivity model using a
317 binomial error structure, the productivity model using a Poisson error structure, and the
318 exploitation rate model using a negative binomial error structure with observation level
319 random effects (M3).

320 Next, we asked whether spatial structure or host heterogeneity have significant effects on viral
321 phenotypes across genotypes (without accounting an effect of specialization). We built models
322 for infectivity, productivity, and composite exploitation with the same random effects as above,
323 and without fixed effects for being assayed on the familiar or foreign host. For host
324 heterogeneity models, we included the assay genotype, food type, and whether the treatment
325 had homogeneous or heterogeneous hosts as fixed effects, allowing for an interaction between
326 food type and treatment heterogeneity (M4). The infectivity model uses a binomial error
327 structure with observation level random effects and the productivity and composite
328 exploitation models use a zero-inflated negative binomial error structure with observation level
329 random effects. For spatial structure models, we include the food type and assay genotype as
330 fixed effects with the same random effects as above (M5). The infectivity model uses a binomial
331 error structure, and the productivity and composite exploitation models use a zero inflated
332 negative binomial structure with observation level random effects.

333 Finally, we asked whether virus phenotypes are spatially structured within the heterogeneous
334 host treatments (M6). First, the local proportion of host genotypes during evolution was
335 determined for each virus population by its distance from the host contact zone so that the
336 edge of the microcosm where host genotype 17 was added was coded as 1, the next row of the
337 grid was coded .75, the middle contact zone was coded as 0.5, the following row was coded as
338 .25, and the edge of the microcosm where host genotype 9 was added was coded as 0. Thus,
339 the inverse represents the local proportion of host genotype 9. We built models for infectivity,
340 productivity, and exploitation rate that included the local proportion of host genotype, the host
341 genotype of the assay, the food type, an interaction effects between these three terms, and the
342 order of genotypes in the microcosm as fixed effects. We included the same random effects as
343 in the previous models for batch and nestedness and also for the specific position. The
344 infectivity model uses a binomial error structure, the productivity model uses a Poisson error
345 structure with observation level random effects, and the exploitation rate model uses a zero-
346 inflated negative binomial error structure.

347

348 **RESULTS**

349 Food viscosity spatially structures infection

350 In our experiments testing how food viscosity affected larval movement, we see that 'sticky'
351 food greatly decreases larval dispersal (Figure 1A, Table S1). In test microcosms where larvae

are only added to one side, the count of individuals found in a grid square after 21 days is significantly affected by the interaction between the distance that the square is from where larvae were added and the food viscosity (MS2 ANOVA $p < 0.001$), with larvae in sticky food dispersing less (MS2 GLMM effect estimate = -3.8, $p < 0.001$). Interestingly, neither the effect of distance ($p = 0.96$) nor food viscosity ($p = 0.07$) significantly affects the count in a grid square alone (MS2 ANOVA).

Across the evolution experiment, microcosms had an average of 199.7 infected cadavers (range 23-626). Treatments with different food viscosities differ in the variance of number of infected cadavers per square ($p < 0.001$, MS1), with 'sticky' food having more clustered infected individuals, indicating more local transmission (Figure 2B).

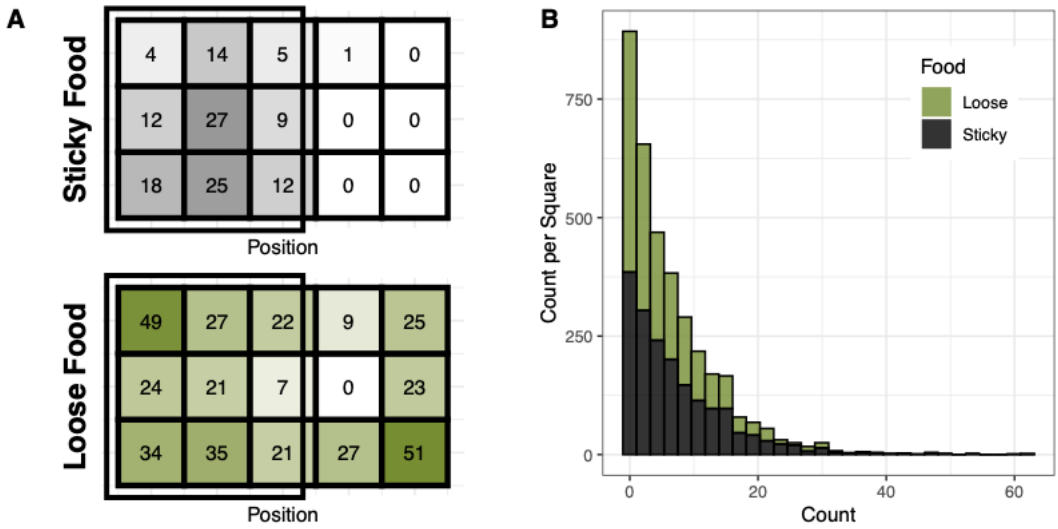

Figure 2: (A) Heatmaps of where individuals are found after 21 days in test microcosms of 'sticky' (top) and 'loose' (bottom) food where food containing larvae has been added to one half of the microcosm (black box) and sterile food to the other. Numbers represent the total number of individuals found in each square. (B) Histogram showing the number of grid squares (y-axis) with different counts of infected larvae (x-axis) during serial passage. Variance is higher in the 'sticky' food condition (MS1).

<u>The impact of specialization on virus phenotypes depends on spatial structure</u>

Without allowing for interaction effects, neither food viscosity (M2c ANOVA $p = 0.8$, M2i ANOVA $p = 0.7$, M2p ANOVA $p = 0.8$) nor being assayed on the familiar or foreign host (M2c ANOVA $p = 0.2$, M2i ANOVA $p = 0.059$, M2p ANOVA $p = 0.7$) significantly affect evolved virus phenotypes in homogeneous microcosms (Figure S5). This is in contrast to previous results from the system that manipulate spatial structure, but only assay on familiar, genetically diverse hosts [30] and that assay on both familiar and foreign hosts, but do not manipulate spatial structure [38].

However, trade-offs associated with virus host range and virus life history strategy may interact to change evolutionarily optimal strategies for a population. When we build models that allow for interactions between spatial structure and host specialization, we see that the effect of

being assayed on the familiar line depends on spatial structure (M3c ANOVA $p = 0.047$, GLMM effect estimate Foreign x Sticky = 0.10 $p = 0.047$) (Figure 3, S4).

Virus populations are significantly less exploitative of their familiar host in loose food (M3c contrasts loose effect estimate = -1.29 $p = 0.03$) and non-significantly more exploitative of their familiar host in sticky food (M3c contrasts sticky effect estimate = 1.02 $p = 0.09$) (Figure 3F). This is largely because of differences in viral productivity (M3p contrasts loose effect estimate = -0.78 $p = 0.03$; sticky effect estimate = 0.442 $p = 0.2$) (Figure 3D), rather than infectivity (M3i contrasts loose effect estimate = -0.24 $p = 0.37$; sticky effect estimate = 0.09 $p = 0.7$) (Figure 3B).

This indicates that the direction of the effect of viral specialization on host exploitation rate varies with population spatial structure.

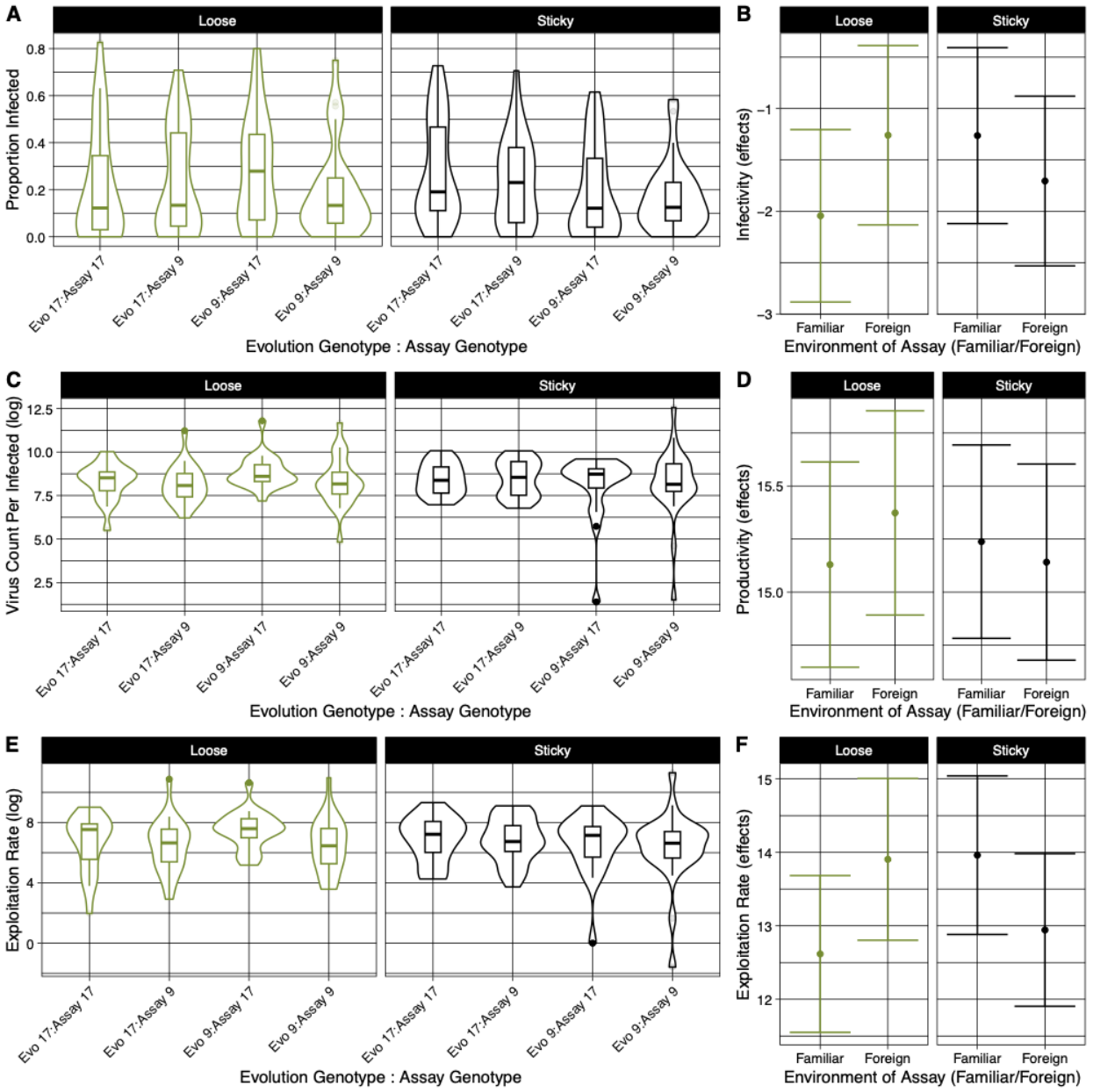

*Figure 3: Interactions between specialization and the spatial structuring of infection in homogeneous microcosms. Panels A, C, E plot raw data and panels B, D, F show model effect estimates drawn from M3 GLMMs. Y-axes represent: (A) proportion infected, (B) effect estimates for the M3i infectivity model, (C) average number of occlusion bodies produced per infectious cadaver on a log scale, (D) effect estimates for the M3p viral productivity model, (E) composite exploitation rate (proportion infected * average number of occlusion bodies) on a log scale, and (F) effect estimates for the M3c exploitation rate model. A, C, E X-axes represent the combinations of which host genotype the virus population evolved on and which they were assayed on. B, D, F X-axes represent whether the virus was being assayed on the host genotype that it evolved on (familiar) or on the foreign host genotype. Panels show whether the virus came from a treatment with 'loose' food or 'sticky' food.*

<u>Spatially structured host genetic diversity leads to local specialization</u>

On average, virus populations evolved in heterogeneous host populations do not significantly differ in infectivity (M4i ANOVA, p = 0.8) or composite exploitation (M4c ANOVA, p=0.12) from those evolved in homogeneous host populations and are slightly more productive (M4p GLMM effect estimate = 0.16 p = 0.04).

However, heterogeneous host populations have gradients of host mixing within them as the different positions are different distances from the other host genotype. Additionally, we expect spatial structure to impede host movement and thus further alter the degree of host mixing for different positions. Therefore, we explore whether there is an effect of host specialization within the heterogeneous host microcosms and whether this effect is altered by the spatial structuring of the population.

We find that, for composite exploitation rate, there is a significant interaction between the local proportion of a host genotype during evolution (i.e. the position's distance from the contact zone), the assay host genotype, and the type of food evolved in (M6c ANOVA p = 0.029, GLMM estimate = 0.56 p = 0.029, Figure 4). This is due to differences in virus productivity (M6p ANOVA p = 0.018), but not infectivity (M6i ANOVA p = 0.60).

The significant interaction between local proportion of a host genotype during evolution, assay host genotype, and food type is driven by populations from sticky food where virus from different positions within the microcosm have higher exploitation rates on their locally familiar host populations (M6c pairwise contrasts effect estimate = 1.7 p = 0.033). In contrast, virus phenotypes within loose food microcosms do not significantly vary, though, like in homogeneous microcosms, they have slightly lower exploitation rates on the familiar host (M6c pairwise contrasts effect estimate = -0.65 p = 0.37). This indicates that spatially structured host heterogeneity results in the evolution of more diverse, locally specialized virus.

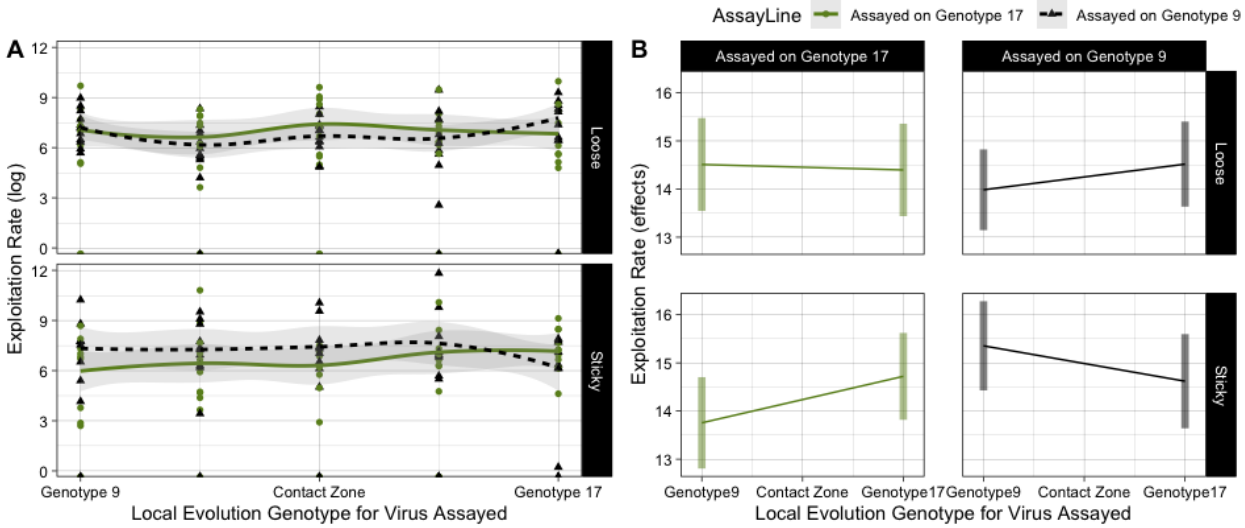

*Figure 4: Spatially structured host heterogeneity results in locally specialized virus. Virus sampled from different spatial positions within each microcosm (along x-axis with tick labels denoting the local evolution host genotype, i.e. Figure 1 vertical axes) were assayed on the two host genotypes. (A) Raw data for the composite exploitation rate (proportion infected * average number of occlusion bodies, log-scale, y-axis) on the two host genotypes (green, circle, solid line is exploitation rate on genotype 17; black, triangle, dashed is on genotype 9) for virus from 'sticky' and 'loose' food microcosms (panels) for virus sampled from different spatial positions within the microcosm (x-*

axis) with therefore different evolutionary histories of mixing between the 2 host genotypes (B) Model effect estimates drawn from M6c GLMM for the interacting effects of food type and assay genotype on exploitation rate (y-axis) for virus sampled from different spatial positions within the microcosm with different degrees of mixing between the 2 host genotypes (x-axis). Panels are separated vertically by food type and horizontally by which host genotype the virus was assayed on.

DISCUSSION

We experimentally evolve baculovirus in microcosms that vary in spatial structure and host genetic diversity to explore how these two selection pressures interact to shape host range evolution. Our experimental evolution approach manipulates the viscosity of the food medium that the moth larvae live within and adds either homogeneous (single inbred line) or heterogeneous (two inbred line) hosts. We then assay virus population from different positions within the microcosm on both the familiar and foreign host. The key result of our experiment is that spatially structured heterogeneous host populations support localized virus specialization and, therefore, more diverse viral strategies within the population. Virus sampled from different positions within heterogeneous microcosms showed higher exploitation rates on the locally dominant host genotype in spatially structured environments but not in well-mixed ones (Figure 4). This finding supports theory suggesting that more contact between host genotypes selects for generalism, while lower contact rates can allow for the persistence of local specialists [20,22]. This implies that the benefits of host genetic diversity in selecting for 'mediocre generalists' and preventing the 'monoculture effect' [2,4,19] may only be realized when host heterogeneity is well-mixed.

A second important result is that we also find that the direction of the effect of specialization on host exploitation rate is reversed depending on spatial structure. Specifically, in both homogeneous and heterogeneous treatments, virus populations had higher exploitation rates on their familiar host in spatially structured microcosms, and lower exploitation rates on their familiar host in well-mixed microcosms (Figure 3). This suggests that spatial structure may be imposing additional selection pressures that are altering the evolutionarily optimal strategy on the familiar host type. However, it can be argued that the direction of the specialization results is counterintuitive. Standard expectations—based on earlier theory and experiments—would predict that well-mixed microcosms should select for increased exploitation of the familiar host, while spatially structured environments might select for more prudent exploitation [27,28,30]. We saw the opposite.

There are several potential explanations for this unexpected result. The first is that some theory suggests that intermediate levels of spatial structure can actually select for higher parasite exploitation rates [28,33]—our sticky food treatment could fall within this range. However, this would not explain why viruses from well-mixed treatments evolved lower exploitation rates on

470 their familiar host. These lower exploitation rates could, however, result from an unmeasured
471 phenotype, such as time to kill, being selected upon and trading off with our measured metrics
472 (infectivity and productivity). In other baculoviruses, shorter time to kill correlates with lower
473 virus productivity [62], so selection for rapid infection cycles could explain the lower
474 exploitation rates we observe in loose food conditions. In addition, another phenotype that we
475 did not measure but that could trade-off with viral infectivity is environmental persistence [63].
476 Finally, it could also be possible that the loose food environment more closely resembled
477 ancestral conditions, resulting in weak selection on exploitation rate, while virus in sticky food
478 experienced stronger selection to increase exploitation on the familiar host. Meanwhile,
479 exploitation of the foreign host may have drifted in opposite directions independently.

480 Our results have implications for broader ecological and evolutionary theory on how
481 specialization supports diversity, as they challenge the general assumption of rare host
482 advantage. In our experiment, pathogens sometimes exhibited (presumably maladaptive) high
483 virulence on foreign hosts, suggesting that rare host genotypes may not always have a fitness
484 advantage. This would complicate many models of host–parasite coevolution—including the
485 Red Queen Hypothesis and Janzen-Connell effects [64–66]—that depend on negative
486 frequency-dependent selection arising from rare host advantage. We find that, under certain
487 spatial and population structures, selection for lower virulence on the familiar host type can
488 make rare hosts more vulnerable to infection. While similar patterns of high foreign host
489 virulence have been noted in contexts such as species invasions (i.e., "invading with weapons")
490 and zoonoses [67,68], those cases are typically attributed to evolved resistance in the familiar
491 host leading to coevolutionary arms races that result in higher foreign host virulence. Our
492 results suggest that such patterns can occur even in the absence of host coevolution. If such
493 reversed specialization emerges regularly under certain ecological conditions, it may violate the
494 assumptions necessary for rare genotype advantage to maintain diversity through negative
495 frequency-dependent selection.

496 In conclusion, our experiment shows that spatial structure and host genetic diversity interact to
497 alter pathogen host range evolution and how pathogens specialize. We demonstrate that
498 spatially structured host heterogeneity can support local specialization, and that the direction
499 of specialization's effect on exploitation rate—whether higher or lower on the familiar host—
500 depends on the population's spatial structure. These findings highlight the importance of
501 multidimensional trade-offs in pathogen evolution, particularly interactions between host
502 range and life-history traits, and suggest that such interactions can produce unexpected and
503 context-dependent outcomes. Finally, this work has important implications for controlling
504 infectious diseases in heterogeneous populations, as spatial structure may limit the
505 effectiveness of host diversity in constraining pathogen adaptation.

506

507 **REFERENCES**

508 1. King KC, Lively CM. 2012 Does genetic diversity limit disease spread in natural host
509 populations? *Heredity* **109**, 199–203. (doi:10.1038/hdy.2012.33)

510 2. Gibson AK. 2022 Genetic diversity and disease: The past, present, and future of an old idea.
511 *Evolution* **76**, 20–36. (doi:10.1111/evo.14395)

512 3. Zhu Y *et al.* 2000 Genetic diversity and disease control in rice. *Nature* **406**, 718–722.
513 (doi:10.1038/35021046)

514 4. Elton CS. 1958 *The ecology of invasions by animals and plants.* Chicago, IL: University of
515 Chicago Press. See https://www.cabdirect.org/cabdirect/abstract/19592202723.

516 5. Ekroth AKE, Rafaluk-Mohr C, King KC. 2019 Host genetic diversity limits parasite success
517 beyond agricultural systems: a meta-analysis. *Proc. R. Soc. B Biol. Sci.* **286**, 20191811.
518 (doi:10.1098/rspb.2019.1811)

519 6. Cornwall DH, Kubinak JL, Zachary E, Stark DL, Seipel D, Potts WK. 2018 Experimental
520 manipulation of population-level MHC diversity controls pathogen virulence evolution in
521 Mus musculus. *J. Evol. Biol.* **31**, 314–322. (doi:10.1111/jeb.13225)

522 7. White PS, Choi A, Pandey R, Menezes A, Penley M, Gibson AK, de Roode J, Morran L. 2020
523 Host heterogeneity mitigates virulence evolution. *Biol. Lett.* **16**, 20190744.
524 (doi:10.1098/rsbl.2019.0744)

525 8. Gibson AK, Nguyen AE. 2021 Does genetic diversity protect host populations from
526 parasites? A meta-analysis across natural and agricultural systems. *Evol. Lett.* **5**, 16–32.
527 (doi:10.1002/evl3.206)

528 9. Hughes WOH, Boomsma JJ. 2004 Genetic Diversity and Disease Resistance in Leaf-Cutting
529 Ant Societies. *Evolution* **58**, 1251–1260. (doi:10.1111/j.0014-3820.2004.tb01704.x)

530 10. González R, Butković A, Elena SF. 2019 Role of host genetic diversity for susceptibility-to-
531 infection in the evolution of virulence of a plant virus. *Virus Evol.* **5**.
532 (doi:10.1093/ve/vez024)

533 11. Kubinak JL, Ruff JS, Hyzer CW, Slev PR, Potts WK. 2012 Experimental viral evolution to
534 specific host MHC genotypes reveals fitness and virulence trade-offs in alternative MHC
535 types. *Proc. Natl. Acad. Sci.* **109**, 3422–3427. (doi:10.1073/pnas.1112633109)

536 12. Ekroth AKE, Gerth M, Stevens EJ, Ford SA, King KC. 2021 Host genotype and genetic
537 diversity shape the evolution of a novel bacterial infection. *ISME J.* **15**, 2146–2157.
538 (doi:10.1038/s41396-021-00911-3)

539 13. Levins R. 1962 Theory of Fitness in a Heterogeneous Environment. I. The Fitness Set and
540 Adaptive Function. *Am. Nat.* **96**, 361–373. (doi:10.1086/282245)

541 14. Fry JD. 1996 The Evolution of Host Specialization: Are Trade-Offs Overrated? *Am. Nat.* **148**,
542 S84–S107.

543 15. Whitlock MC. 1996 The Red Queen Beats the Jack-Of-All-Trades: The Limitations on the
544 Evolution of Phenotypic Plasticity and Niche Breadth. *Am. Nat.* **148**, S65–S77.

545 16. Regoes RR, Nowak MA, Bonhoeffer S. 2000 Evolution of Virulence in a Heterogeneous Host
546 Population. *Evolution* **54**, 64–71. (doi:10.1111/j.0014-3820.2000.tb00008.x)

547 17. Kawecki TJ. 1994 Accumulation of Deleterious Mutations and the Evolutionary Cost of Being
548 a Generalist. *Am. Nat.* **144**, 833–838.

549 18. Bono LM, Draghi JA, Turner PE. 2019 Evolvability Costs of Niche Expansion. *Trends Genet.* **0**.
550 (doi:10.1016/j.tig.2019.10.003)

551 19. Visher E, Boots M. 2020 The problem of mediocre generalists: population genetics and eco-
552 evolutionary perspectives on host breadth evolution in pathogens. *Proc. R. Soc. B Biol. Sci.*
553 **287**, 20201230. (doi:10.1098/rspb.2020.1230)

554 20. Gandon S, Poulin R. 2004 Evolution of multihost parasites. *Evolution* **58**, 455–469.
555 (doi:10.1554/03-390)

556 21. Osnas EE, Dobson AP. 2012 Evolution of Virulence in Heterogeneous Host Communities
557 Under Multiple Trade-Offs. *Evolution* **66**, 391–401. (doi:10.1111/j.1558-5646.2011.01461.x)

558 22. Williams PD. 2012 New Insights into Virulence Evolution in Multigroup Hosts. *Am. Nat.* **179**,
559 228–239. (doi:10.1086/663690)

560 23. Gandon S. 2002 Local adaptation and the geometry of host–parasite coevolution. *Ecol. Lett.*
561 **5**, 246–256. (doi:10.1046/j.1461-0248.2002.00305.x)

562 24. Gandon S, Capowiez Y, Dubois Y, Michalakis Y, Olivieri I. 1996 Local adaptation and gene-
563 for-gene coevolution in a metapopulation model. *Proc R Soc Lond B* **263**, 1003–1009.
564 (doi:10.1098/rspb.1996.0148)

565 25. Gandon S, Michalakis Y. 2002 Local adaptation, evolutionary potential and host–parasite
566 coevolution: interactions between migration, mutation, population size and generation
567 time. *J. Evol. Biol.* **15**, 451–462. (doi:10.1046/j.1420-9101.2002.00402.x)

568 26. Boots M, Sasaki A. 2000 The evolutionary dynamics of local infection and global
569 reproduction in host-parasite interactions. *Ecol. Lett.* **3**, 181–185.

570 27. Boots M, Sasaki A. 1999 'Small worlds' and the evolution of virulence: infection occurs
571 locally and at a distance. *Proc. R. Soc. B Biol. Sci.* **266**, 1933–1938.

572 28. Lion S, Boots M. 2010 Are parasites '"prudent"' in space? *Ecol. Lett.* **13**, 1245–1255.
573 (doi:10.1111/j.1461-0248.2010.01516.x)

574 29. Messinger SM, Ostling A. 2009 The Consequences of Spatial Structure for the Evolution of
575 Pathogen Transmission Rate and Virulence. *Am. Nat.* **174**, 441–454. (doi:10.1086/605375)

576 30. Boots M, Mealor M. 2007 Local Interactions Select for Lower Pathogen Infectivity. *Science*
577 **315**, 1284–1286. (doi:10.1126/science.1137126)

578 31. Kerr B, Neuhauser C, Bohannan BJM, Dean AM. 2006 Local migration promotes competitive
579 restraint in a host–pathogen 'tragedy of the commons'. *Nature* **442**, 75–78.
580 (doi:10.1038/nature04864)

581 32. Berngruber TW, Lion S, Gandon S. 2015 Spatial Structure, Transmission Modes and the
582 Evolution of Viral Exploitation Strategies. *PLOS Pathog.* **11**, e1004810.
583 (doi:10.1371/journal.ppat.1004810)

584 33. Kamo M, Sasaki A, Boots M. 2007 The role of trade-off shapes in the evolution of parasites
585 in spatial host populations: An approximate analytical approach. *J. Theor. Biol.* **244**, 588–
586 596. (doi:10.1016/j.jtbi.2006.08.013)

587 34. van Baalen M. 2002 Contact Networks and the Evolution of Virulence. In *Adaptive Dynamics*
588 *of Infectious Diseases: In Pursuit of Virulence Management*, Cambridge: Cambridge
589 University Press.

590 35. Amado A, Campos PRA. 2019 Ecological specialization under multidimensional trade-offs.
591 *Evol. Ecol.* **33**, 769–789. (doi:10.1007/s10682-019-10013-4)

592 36. Cressler CE, King AA, Werner EE. 2010 Interactions between Behavioral and Life-History
593 Trade-Offs in the Evolution of Integrated Predator-Defense Plasticity. *Am. Nat.* **176**, 276–
594 288. (doi:10.1086/655425)

595 37. Edwards KF, Klausmeier CA, Litchman E. 2011 Evidence for a three-way trade-off between
596 nitrogen and phosphorus competitive abilities and cell size in phytoplankton. *Ecology* **92**,
597 2085–2095. (doi:10.1890/11-0395.1)

598 38. Visher E, Uricchio L, Bartlett L, DeNamur N, Yarcan A, Alhassani D, Boots M. 2022 The
599 evolution of host specialization in an insect pathogen. *Evolution* **76**, 2375–2388.
600 (doi:10.1111/evo.14594)

601 39. Boots M, Childs D, Crossmore J, Tidbury H, Rudolf V. 2021 Experimental evidence that local
602 interactions select against selfish behaviour. *Ecol. Lett.* **24**, 1187–1192.
603 (doi:10.1111/ele.13734)

604 40. Boots M, Childs D, Reuman DC, Mealor M. 2009 Local Interactions Lead to Pathogen-Driven
605 Change to Host Population Dynamics. *Curr. Biol.* **19**, 1660–1664.
606 (doi:10.1016/j.cub.2009.07.070)

607 41. Gage MJ. 1995 Continuous variation in reproductive strategy as an adaptive response to
608 population density in the moth Plodia interpunctella. *Proc. R. Soc. Lond. B Biol. Sci.* **261**, 25–
609 30. (doi:10.1098/rspb.1995.0112)

610 42. Mohandass S, Arthur FH, Zhu KY, Throne JE. 2007 Biology and management of Plodia
611 interpunctella (Lepidoptera: Pyralidae) in stored products. *J. Stored Prod. Res.* **43**, 302–311.
612 (doi:10.1016/j.jspr.2006.08.002)

613 43. Consigli RA, Tweeten KA, Anderson DK, Bulla LA. 1983 Granulosis Viruses, with Emphasis on
614 the Gv of the Indian Meal Moth, Plodia interpunctella. In *Advances in Virus Research* (eds
615 MA Lauffer, K Maramorosch), pp. 141–173. Academic Press. (doi:10.1016/S0065-
616 3527(08)60723-X)

617 44. Harrison RL, Rowley DL, Funk CJ. 2016 The Complete Genome Sequence of Plodia
618 Interpunctella Granulovirus: Evidence for Horizontal Gene Transfer and Discovery of an
619 Unusual Inhibitor-of-Apoptosis Gene. *PLoS ONE* **11**, e0160389.
620 (doi:10.1371/journal.pone.0160389)

621 45. Tidbury H. 2012 The Evolutionary Ecology of Antiviral Resistance in Insects. phd, University
622 of Sheffield. See http://etheses.whiterose.ac.uk/2937/.

623 46. Begon M, Daud KBH, Young P, Howells RE. 1993 The Invasion and Replication of a
624 Granulosis Virus in the Indian Meal Moth, Plodia interpunctella: An Electron Microscope
625 Study. *J. Invertebr. Pathol.* **61**, 281–295. (doi:10.1006/jipa.1993.1053)

626 47. Bartlett LJ, Wilfert L, Boots M. 2018 A genotypic trade-off between constitutive resistance
627 to viral infection and host growth rate. *Evolution* **72**, 2749–2757. (doi:10.1111/evo.13623)

628 48. Bartlett LJ, Visher E, Haro Y, Roberts KE, Boots M. 2020 The target of selection matters: An
629 established resistance—development-time negative genetic trade-off is not found when
630 selecting on development time. *J. Evol. Biol.* **33**, 1109–1119. (doi:10.1111/jeb.13639)

631 49. Oppert B, Hammel R, Throne JE, Kramer KJ. 2000 Fitness costs of resistance to Bacillus
632 thuringiensis in the Indianmeal moth, Plodia interpunctella. *Entomol. Exp. Appl.* **96**, 281–
633 287. (doi:10.1046/j.1570-7458.2000.00707.x)

634 50. Bolker BM, Brooks ME, Clark CJ, Geange SW, Poulsen JR, Stevens MHH, White J-SS. 2009
635 Generalized linear mixed models: a practical guide for ecology and evolution. *Trends Ecol.*
636 *Evol.* **24**, 127–135. (doi:10.1016/j.tree.2008.10.008)

637 51. R Core Team. 2021 *R: A language and environment for statistical computing.* Vienna,
638 Austria: R Foundation for Statistical Computing. See https://www.r-project.org/.

52. Bates D, Mächler M, Bolker B, Walker S. 2015 Fitting Linear Mixed-Effects Models Using lme4. *J. Stat. Softw.* **67**, 1–48. (doi:10.18637/jss.v067.i01)

53. Brooks ME, Kristensen K, Benthem KJ van, Magnusson A, Berg CW, Nielsen A, Skaug HJ, Mächler M, Bolker BM. 2017 glmmTMB Balances Speed and Flexibility Among Packages for Zero-inflated Generalized Linear Mixed Modeling. *R J.* **9**, 378–400.

54. Fox J, Weisberg S. 2019 *An R Companion to Applied Regression, 3rd Edition*. See https://socialsciences.mcmaster.ca/jfox/Books/Companion/index.html.

55. Hartig F, Lohse L. 2021 DHARMa: Residual Diagnostics for Hierarchical (Multi-Level / Mixed) Regression Models.

56. Lenth RV, Buerkner P, Herve M, Love J, Miguez F, Riebl H, Singmann H. 2022 emmeans: Estimated Marginal Means, aka Least-Squares Means.

57. Pedersen TL. 2020 patchwork: The Composer of Plots.

58. Singmann H *et al.* 2019 afex: Analysis of Factorial Experiments.

59. Wickham H. 2009 *ggplot2 - Elegant Graphics for Data Analysis*. Springer. See https://www.springer.com/gp/book/9780387981413.

60. Wickham H *et al.* 2019 Welcome to the Tidyverse. *J. Open Source Softw.* **4**, 1686. (doi:10.21105/joss.01686)

61. Harrison XA. 2014 Using observation-level random effects to model overdispersion in count data in ecology and evolution. *PeerJ* **2**, e616. (doi:10.7717/peerj.616)

62. Cooper VS, Reiskind MH, Miller JA, Shelton KA, Walther BA, Elkinton JS, Ewald PW. 2002 Timing of transmission and the evolution of virulence of an insect virus. *Proc. Biol. Sci.* **269**, 1161–1165. (doi:10.1098/rspb.2002.1976)

63. Ogbunugafor CB, Alto BW, Overton TM, Bhushan A, Morales NM, Turner PE. 2013 Evolution of Increased Survival in RNA Viruses Specialized on Cancer-Derived Cells. *Am. Nat.* **181**, 585–595. (doi:10.1086/670052)

64. Janzen DH. 1970 Herbivores and the Number of Tree Species in Tropical Forests. *Am. Nat.* **104**, 501–528. (doi:10.1086/282687)

65. Connell JH. 1971 On the role of natural enemies in preventing competitive exclusion in some marine animals and in rain forest trees. *Dyn. Popul.* **298**, 312.

66. Jaenike J. 1978 A hypothesis to account for the maintenance of sex within populations. *Evol Theory* **3**, 191–194.

670 67. Tompkins DM, White AR, Boots M. 2003 Ecological replacement of native red squirrels by
671 invasive greys driven by disease. *Ecol. Lett.* **6**, 189–196. (doi:10.1046/j.1461-
672 0248.2003.00417.x)

673 68. Guth S, Visher E, Boots M, Brook CE. 2019 Host phylogenetic distance drives trends in virus
674 virulence and transmissibility across the animal–human interface. *Philos. Trans. R. Soc. B*
675 *Biol. Sci.* **374**, 20190296. (doi:10.1098/rstb.2019.0296)

676
677
678
679
680
681
682
683
684
685
686
687
688
689